

Dynamic Assembly/Disassembly Processes of Photoresponsive DNA Origami Nanostructures Directly Visualized on a Lipid Membrane Surface

Yuki Suzuki,^{†,§} Masayuki Endo,^{*,‡,§} Yangyang Yang,[†] and Hiroshi Sugiyama^{*,†,‡,§}

[†]Department of Chemistry, Graduate School of Science, Kyoto University, Kitashirakawa-oiwakecho, Sakyo-ku, Kyoto 606-8502, Japan

[‡]Institute for Integrated Cell-Material Sciences (WPI-iCeMS), Kyoto University, Yoshida-ushinomiya-cho, Sakyo-ku, Kyoto 606-8501, Japan

[§]CREST, Japan Science and Technology Corporation (JST), Sanbancho, Chiyoda-ku, Tokyo 102-0075, Japan

Supporting Information

ABSTRACT: Here, we report the direct visualization of the assembly/disassembly processes of photoresponsive DNA origami nanostructures which can be placed on a lipid bilayer surface. The observation relies on controlled interactions between the bilayer components and cholesterol moieties introduced to the hexagonal origami structures, one of whose outer edges carries Azo-ODNs. The bilayer-placed hexagonal dimer was disassembled into monomer units by UV irradiation, and reversibly assembled again during visible light irradiation. These dynamic processes were directly monitored with high-speed atomic force microscopy. The successful application of our approach should facilitate studies of interactive and functional behaviors of various DNA nanostructures.

A programmed self-assembly of nanostructural units into organized structure is a fundamental key process for the bottom-up construction of nano/microscale products.^{1–3} For the precise construction of such products in a programmed fashion, analysis of the assembling and disassembling processes is required. The assembled products are now commonly visualized by atomic force microscopy (AFM) or electron microscopy (EM) with nanoscale resolution. However, these imaging techniques rely on an immobilization of pre-assembled samples onto a substrate surface. Thus, direct visualization of the interactive behavior of the nanostructural units remains a major challenge.

In this study, we aimed to directly visualize assembly/disassembly processes of photoresponsive DNA origami nanostructures⁴ using high-speed atomic force microscopy (HS-AFM) imaging technique.^{5,6} Success in time-lapse imaging by HS-AFM requires conditions which satisfy two conflicting requirements: (i) adsorption of structures of interest onto a substrate surface, and concurrently, (ii) assuring sufficient mobility of the structures to allow their function-related conformational/morphological changes. To achieve those conditions, we here employed sphingomyelin (SM)-enriched domains in a phase-separated bilayer^{7–10} as imaging substrates, on which cholesterol-TEG modified DNA nanostructures can be adsorbed with moderate mobility.

The derivative of the previously reported hexagonal DNA origami unit⁴ was used with an incorporation of cholesterol-TEG modified staples (Figure 1a). Six cholesterol moieties were introduced to the same face (bottom-face) of the origami in symmetrical positions so that each domain has one cholesterol moiety. Two pseudocomplementary photoresponsive short oligodeoxynucleotides (ODNs), Azo-ODN1 and Azo-ODN2, containing different numbers of *trans*-form azobenzene moieties were also introduced to the staples on the outer 'd-edge' of the hexagonal DNA origami structures (Figure 1a,b). These Azo-ODNs form duplex in *trans*-form under vis irradiation and dissociate in *cis*-form under UV irradiation by reversible *trans*–*cis* photoisomerization.^{11–14} Hence, the assembly and disassembly of the dimer of hexagonal structure at the d-edge can be controlled by appropriate photoirradiation.⁴ Two monomer units Hx1 and Hx2 were created by modifying their d-edge with four Azo-ODN1 strands and four Azo-ODN2 strands, respectively (Figure 1b). Each of the Azo-ODN1 strands carries three azobenzene molecules, while each of the Azo-ODN2 strands contains four azobenzene molecules.

First, we analyzed the constructed cholesterol-modified hexagonal structures on a bare mica surface. AFM images of the monomer units (Hx1 and Hx2) revealed a clear hexagonal shape and homogeneity of the assembled structures without aggregation (Figure 1c, see also Figure S1). The hexagonal dimer was assembled by annealing Hx1 and Hx2 from 50 to 15 °C at a rate of –0.5 °C/min. Gel electrophoresis analysis revealed that the Hx1 and Hx2 effectively interacted one another to form the dimer (Figure S2). AFM imaging of the annealed mixture showed large population (~80%) of interlinked two hexagonal structures (Figure 1d, see also Figure S1). Relative orientation of the hexagonal units in the linked structure was distinguishable by the positions of the small rectangle at the inner side of e-domain (Figure 1d). In the highly magnified image, four short connecting duplexes were clearly visualized in between the d-edges of the hexagons, representing the pseudocomplementary hybridization of ODNs. Thus, it is conceivable that imaged structures are not

Received: October 28, 2013

Published: January 15, 2014

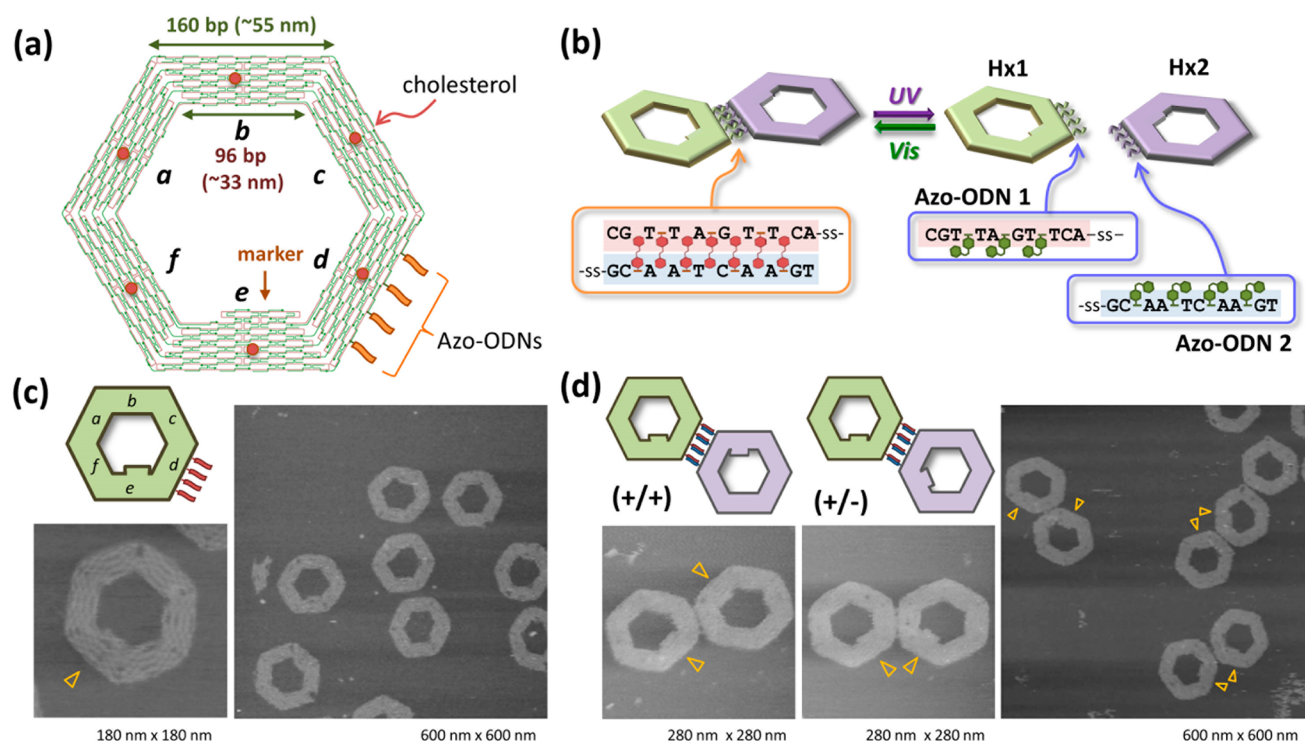


Figure 1. Photoresponsive hexagonal DNA origami structure. (a) Design of the hexagonal unit (top view). Four azobenzene-modified oligonucleotides (Azo-ODN) are introduced into the outer d-edge in counterclockwise order. Each domain (*a–f*) carries one cholesterol-TEG modified staple strand (red filled circle). Cholesterol moieties are placed on the bottom-face of the origami. (b) Schematic illustration of the reversible photoresponsive assembly and disassembly of the hexagonal dimer. (c) AFM images of the assembled monomer. The orientation marker at the inner *e*-edge was indicated by orange triangle. (d) AFM images of assembled dimers. Two different facing orientations of two monomers result in two different types of dimer. The facing orientations of two monomers are distinguishable by the position of the markers (orange triangles).

the hexagonal units just adsorbed adjacent to each other on the mica surface but the dimer selectively connected at the *d*-edges by photoresponsive ODNs. As reported in our previous paper,⁴ two types of hexagonal dimer [i.e., the dimer in the same facing orientation (+/+) and that in the relatively opposite orientation (+/-)] were obtained. Furthermore, population changes in dimer and monomer upon a set of UV/vis irradiation showed clear responses (Figures S2, S3 and Table S1), which are also comparable to our previous results for noncholesterol-modified structures.⁴ Note that any considerable changes in the appearance of the monomer unit were not observed in the AFM images for the UV-irradiated sample (Figure S3), implying that the photoirradiation conditions used in this study is weak enough to avoid damage to the DNA origami structure. Taken together, these results indicate that the staple modification with cholesterol has no effect on the formation of the hexagonal dimer and its reversible photoresponsive behavior.

We next investigated distribution features of the constructed Hx1–Hx2 dimers on a phase-separated supported lipid bilayer which comprised of SM-rich (liquid-ordered) and diolroyl-phosphatidylcholine (DOPC)-rich (liquid-disorderd) phases. AFM imaging of the prepared bilayer revealed a smooth layer of thickness ~4 nm, as expected for a single bilayer (Figure 2a).¹⁵ Furthermore, areas raised ~1 nm above the level of the bilayer were observed, representing a previously reported SM-rich domains.⁹ Because sphingolipids typically have long saturated acyl chains that facilitate close packing, SM enriched domain in a bilayer becomes thicker than areas enriched in more fluidic unsaturated lipids, such as DOPC.

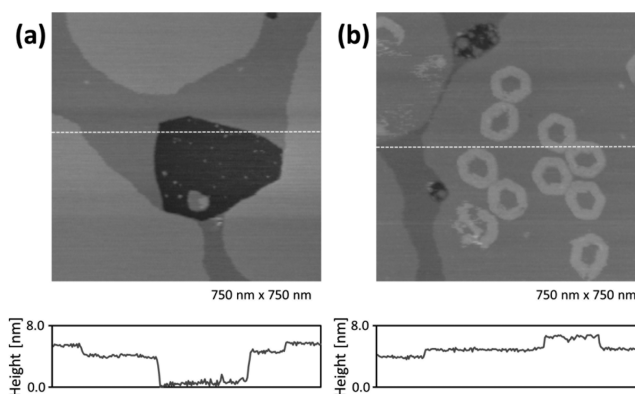


Figure 2. Adsorption of cholesterol–modified hexagonal dimers onto a mica supported lipid bilayer (SLB). Typical AFM image of a SLB either (a) before or (b) after addition of the hexagonal dimers. (Lower panels) Section through the bilayers taken at the positions indicated (lines).

The predimerized Hx1–Hx2 structures were then loaded onto a preformed bilayer. After incubation and subsequent washing step to remove excess volume of origami structures, the bilayer surface was imaged by AFM. Hexagonal shapes preferably appeared on the SM-rich domains (Figures 2b and S4). A section through the origami revealed a height above the SM-rich domain of ~2 nm (Figure 2b) which is consistent with the expected value for DNA origami. Both (+/+) and (+/-) orientations were observed on the bilayer because at least one of the cholesterol modified faces can be in contact with the bilayer surface even in the (+/-) orientation (Figure S4).

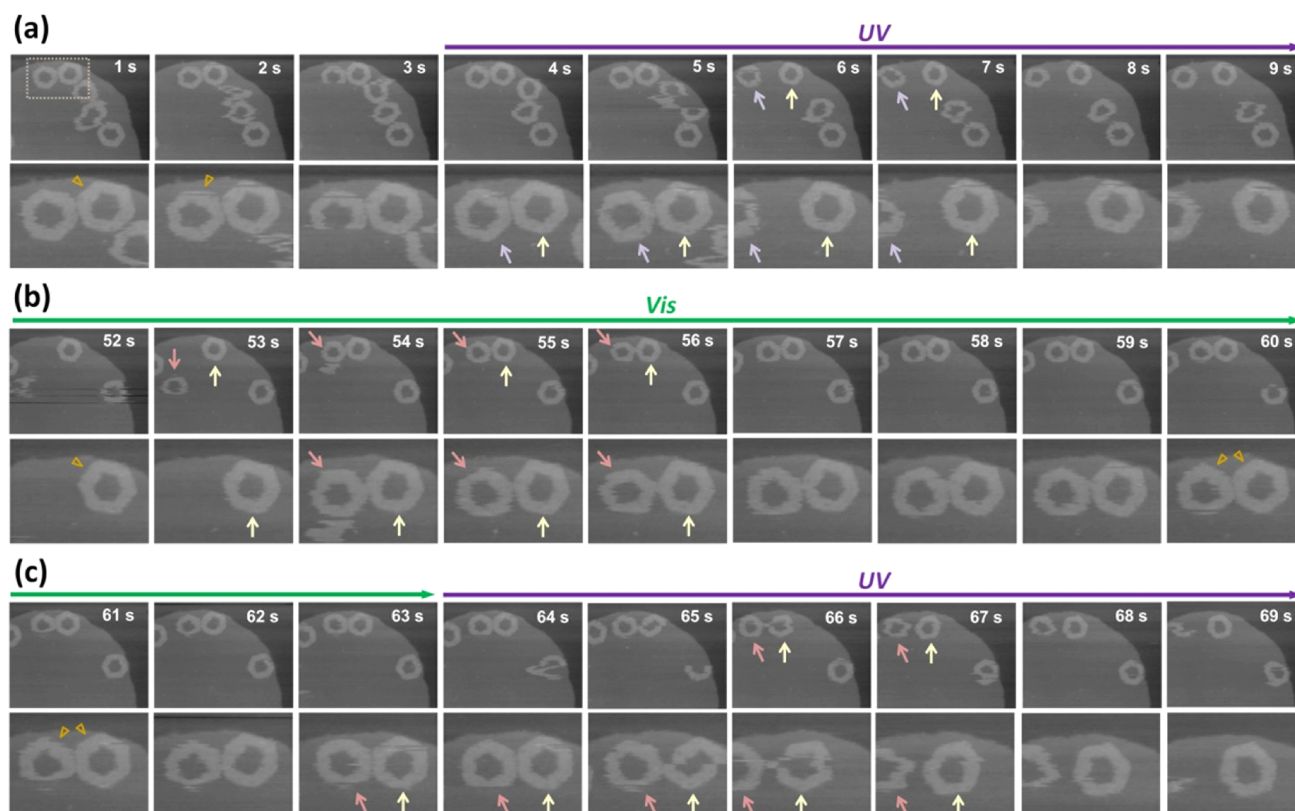


Figure 3. Reversible photoresponsive behavior of hexagonal origami units on a SM-rich domain of a SLB. Time-lapse images were obtained at 1 frame/s, using high-speed AFM. Disassembly/reassembly events were monitored by alternating UV and vis irradiation. The images for the area indicated by dashed line in the first frame are enlarged and shown in lower panels. (a) Disassembly of the hexagonal dimer upon UV irradiation. (b) Reassembly of the hexagonal dimer under vis irradiation. (c) Disassembly event imaged upon second UV irradiation. Image size = 755 nm \times 573 nm (upper panels) and 360 nm \times 300 nm (lower panels). For the complete movie, see Movie S2.

We first tried to follow UV-induced disassembly process of the (+/+)-dimer. Figure S5 shows a series of time-lapse AFM images of a (+/+)-dimer that were observed to dissociate into two monomer units after UV irradiation (see also Movie S1). The dimer unit located on a SM-rich domain was in expected facing-up orientation. After the irradiation with UV at 9 s, the interface of the two d-edges was observed to split, indicating UV-induced dissociation of Azo-ODNs. Before being clearly separated at 62 s, two monomer units were imaged to be adjacent to each other, changing their relative positions. This result shows that both the facing-up units can stay on the SM-rich regions but retain enough mobility on there to allow observation of UV-induced dissociation.

Considering the interaction features of a (+/-)-dimer, in which only one of the units is anchored to the SM molecules, UV irradiation of the (+/-)-dimer trapped on the SM-rich domain would result in the release of the one diffusive monomer. Thus, we next focused on a (+/-)-dimer to capture its dynamic disassembly/reassembly processes. Consecutive HS-AFM imaging successfully monitored this photoresponsive disassembly of a hexagonal dimer (Figure 3a, see also Movie S2). Triangles in initial and second frame of Figure 3a shows the adsorbed dimer is in the (+/-) orientation. At 4 s, the imaging area was irradiated with UV, resulting in the disassembly of the dimer. The monomer unit which indicated by blue arrow was observed to dissociate at 6 s and diffused away from the imaging area, while the other unit (red arrow) remained on the almost same position. Note that the unit

which remained was in facing-up orientation, suggesting its cholesterol-mediated anchoring to the bilayer.

Reassembly process was also captured by subsequently irradiating the same imaging area with visible light (Figure 3b). The vis irradiation was started from 29 s. At 53 s, the monomer unit indicated by green arrow came into the imaging area and contacted with the remained unit (white arrow). From 54 to 56 s, the two units were seen to be touching each other at the corners between d- and e-edges of the hexagonal shape. In the subsequent few frames, the angle between two d-edges was getting narrower. Then, at 60 s, the two units were observed to be connected at the d-edges to form (+/-)-dimer, indicating the photoresponsive dimerization mediated by pseudocomplementary hybridizations of Azo-ODN1s and Azo-ODN2s. Because collision of two units at around d-edges is prerequisite for the dimerization, imaging of the assembly process required longer observation time to catch such occasional events.

The second round of the UV irradiation from 64 s again resulted in the separation of this dimer into monomer units (Figure 3c). Similarly to the result of the first UV irradiation, the unit in facing-up orientation (red arrow) stayed almost in the same area, while the other unit in facing-down orientation (green arrow) was relatively mobile on the surface. These set of results clearly demonstrate that disassembly and reassembly of photoresponsive hexagonal dimer can be directly monitored on the lipid bilayer surface.

In conclusion, we have successfully visualized the dynamic processes of the light-inducible assembly/disassembly of azobenzene-modified DNA origami units using the high-

speed AFM imaging technique. To our knowledge, this is the first report on the real-time imaging of the nano/mesoscale interactive behaviors of 2D DNA origami nanostructural units. It is also noteworthy that the assembly/disassembly of the photoresponsive DNA nanostructures can be regulated on a lipid membrane surface. Recently, a variety of lipid-anchored¹⁶ or membrane-spanning DNA nanostructures^{17–19} have been demonstrated. We add the photocontrollable DNA origami system to this growing list. Our primary results would open up broad perspectives not only for visualization of self-assembly processes but also for construction of functional DNA nanodevices that can be placed on cell membrane surfaces.

■ ASSOCIATED CONTENT

📄 Supporting Information

Experimental procedures, additional figures and movies. This material is available free of charge via the Internet at <http://pubs.acs.org>.

■ AUTHOR INFORMATION

Corresponding Authors

endo@kuchem.kyoto-u.ac.jp

hs@kuchem.kyoto-u.ac.jp

Notes

The authors declare no competing financial interest.

■ ACKNOWLEDGMENTS

This work was supported by Core Research for Evolutional Science and Technology (CREST) of JST and JSPS KAKENHI (Grant Numbers 24310097, 24225005, 24104002). Financial supports from The Mitsubishi Foundation and The Asahi Glass Foundation to M.E. are also acknowledged.

■ REFERENCES

- (1) Park, S. Y.; Lytton-Jean, A. K.; Lee, B.; Weigand, S.; Schatz, G. C.; Mirkin, C. A. *Nature* **2008**, *451*, 553.
- (2) Seeman, N. C. *Nature* **2003**, *421*, 427.
- (3) Whitesides, G. M.; Kriebel, J. K.; Mayers, B. T. In *Nanoscale Assembly*; Huck, W. T. S., Ed.; Springer: New York: 2005, p 217.
- (4) Yang, Y.; Endo, M.; Hidaka, K.; Sugiyama, H. *J. Am. Chem. Soc.* **2012**, *134*, 20645.
- (5) Ando, T.; Kodera, N.; Takai, E.; Maruyama, D.; Saito, K.; Toda, A. *Proc. Natl. Acad. Sci. U.S.A.* **2001**, *98*, 12468.
- (6) Uchihashi, T.; Kodera, N.; Ando, T. *Nat. Protoc.* **2012**, *7*, 1193.
- (7) Yuan, C.; Furlong, J.; Burgos, P.; Johnston, L. J. *Biophys. J.* **2002**, *82*, 2526.
- (8) Saslowsky, D. E.; Lawrence, J.; Ren, X.; Brown, D. A.; Henderson, R. M.; Edwardson, J. M. *J. Biol. Chem.* **2002**, *277*, 26966.
- (9) Lawrence, J. C.; Saslowsky, D. E.; Edwardson, J. M.; Henderson, R. M. *Biophys. J.* **2003**, *84*, 1827.
- (10) Kahya, N.; Scherfeld, D.; Bacia, K.; Poolman, B.; Schwille, P. *J. Biol. Chem.* **2003**, *278*, 28109.
- (11) Asanuma, H.; Liang, X.; Nishioka, H.; Matsunaga, D.; Liu, M.; Komiyama, M. *Nat. Protoc.* **2007**, *2*, 203.
- (12) Endo, M.; Yang, Y.; Suzuki, Y.; Hidaka, K.; Sugiyama, H. *Angew. Chem., Int. Ed.* **2012**, *51*, 10518.
- (13) Liang, X.; Mochizuki, T.; Asanuma, H. *Small* **2009**, *5*, 1761.
- (14) Tanaka, F.; Mochizuki, T.; Liang, X.; Asanuma, H.; Tanaka, S.; Suzuki, K.; Kitamura, S.; Nishikawa, A.; Ui-Tei, K.; Hagiya, M. *Nano Lett.* **2010**, *10*, 3560.
- (15) Sprong, H.; van der Sluijs, P.; van Meer, G. *Nat. Rev. Mol. Cell Biol.* **2001**, *2*, 504.
- (16) Borjesson, K.; Lundberg, E. P.; Woller, J. G.; Norden, B.; Albinsson, B. *Angew. Chem., Int. Ed.* **2011**, *50*, 8312.
- (17) Langecker, M.; Arnaut, V.; Martin, T. G.; List, J.; Renner, S.; Mayer, M.; Dietz, H.; Simmel, F. C. *Science* **2012**, *338*, 932.
- (18) Burns, J. R.; Stulz, E.; Howorka, S. *Nano Lett.* **2013**, *13*, 2351.
- (19) Burns, J. R.; Gopfrich, K.; Wood, J. W.; Thacker, V. V.; Stulz, E.; Keyser, U. F.; Howorka, S. *Angew. Chem., Int. Ed.* **2013**, *52*, 12069.